

# Typical Day Prediction Model for Output Power and Energy Efficiency of a Grid-Connected Solar Photovoltaic System

Yan Su and L. C. Chan

**Abstract**—A novel typical day prediction model have been built and validated by the measured data of a grid-connected solar photovoltaic (PV) system in Macau. Unlike conventional statistical method used by previous study on PV systems which get results by averaging nearby continuous points, the present typical day statistical method obtain the value at every minute in a typical day by averaging discontinuous points at the same minute in different days. This typical day statistical method based on discontinuous point averaging makes it possible for us to obtain the Gaussian shape dynamical distributions for solar irradiance and output power in a yearly or monthly typical day. Based on the yearly typical day statistical analysis results, the maximum possible accumulated output energy in a year with on site climate conditions and the corresponding optimal PV system running time are obtained. Periodic Gaussian shape prediction models for solar irradiance, output energy and system energy efficiency have been built and their coefficients have been determined based on the yearly, maximum and minimum monthly typical day Gaussian distribution parameters, which are obtained from iterations for minimum Root Mean Squared Deviation (RMSD). With the present model, the dynamical effects due to time difference in a day are kept and the day to day uncertainty due to weather changing are smoothed but still included. The periodic Gaussian shape correlations for solar irradiance, output power and system energy efficiency have been compared favorably with data of the PV system in Macau and proved to be an improvement than previous models.

**Keywords**—Grid Connected, RMSD, Solar PV System, Typical Day.

## I. INTRODUCTION

Solar photovoltaic (PV) systems are one kind of the most promising renewable energy systems, and the compounded growth rate is over 15% per annum in the last two decades [1], [2]. Recently, prediction and optimization of output energy and system efficiency for grid-connected solar PV systems attract more and more attentions due to its essential reference values on maintaining the actual load stability of the grid-connected power system [3] and on the design of solar PV power systems [4], [5].

Generally speaking, there are two frequently used approach methods on the study of output power prediction of a grid-connected PV system. One method is based on space angle and extraterrestrial solar radiation calculations, i.e. calculation solar irradiance based on the solar azimuth angle or the zenith angle with a estimated solar constant [6]–[8]. In this method,

people put emphasis on modeling decay functions with maximum at noon and adjusting some coefficients to change the amplitude of predicted solar irradiance of a clear day to match the measured data such as [9], [10]. The limitation of this method is on the difficulty to find a simple practical way to adjust the coefficients to match the difference between the dynamical real weather conditions and a clear day model which are fitful for various places in the world. The other method is based on statistical study on measured data on site of solar PV systems [4], [11]. Because the measured solar irradiance and output energy change dramatically with time in a day, usually daily or monthly averaged solar radiation energy and output energy are calculated to get a monthly distribution of energy output in a year as presented in [12], [13]. This kind of statistical analysis can gives out the real averaged monthly values of solar irradiance and output power on site of the studied solar PV system [14], [15]. However, the daily averaging based statistical method lost the changing infirmation due to time difference in a day. So it can not afford dynamical distributions of solar irradiance and output power in a day.

As discussed above, either one of the above two frequently used methods has its inherent limitations to prediction solar irradiance for real grid-connected solar PV systems in different site on the earth. How to build a uniform practical prediction model which can show both the changes due to time difference in a day and the changes of month to month over a year including the weather effects for solar irradiance, output power and the corresponding system energy efficiency of a solar PV system seems to be a challenge problem, and this inspires the present study.

In this paper, we would like to introduce a novel prediction mode based on a new statistical analysis method which can show the dynamical changing information in a typical day and the month to month tendency at the same time.

## II. PV SYSTEM DESCRIPTION

Before the discussion on our prediction model, we would like to present information of the measured PV system. The present 2.1 kW grid-connected PV system is sited Coloane island of Macau Special Administrative Region, China. The latitude and longitude of Macau city is: 22°10'0"N/113°33'0"E. It is composed by 12 pieces of Ho Tin solar module HTS-175 and the dimensions of each module are 1290×990×36

Yan Su and L. C. Chan are with the Department of Electromechanical Engineering, Faculty of Science and Technology, University of Macau, Taipa, Macau, China. Corresponding author: Yan Su e-mail: (yansu@umac.mo).

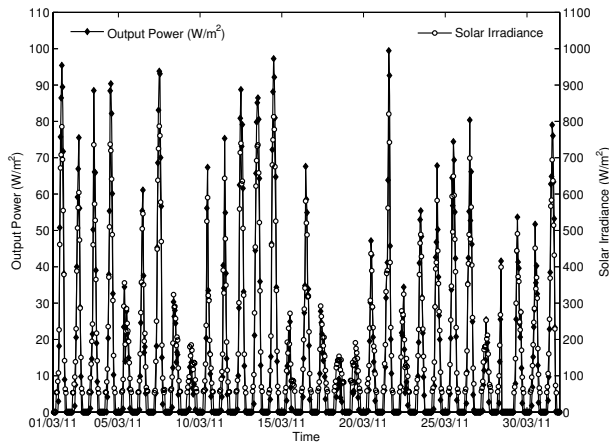


Fig. 1 Hourly Averaged Solar Irradiance and Output Power from 01/03/2011 to 31/03/2011

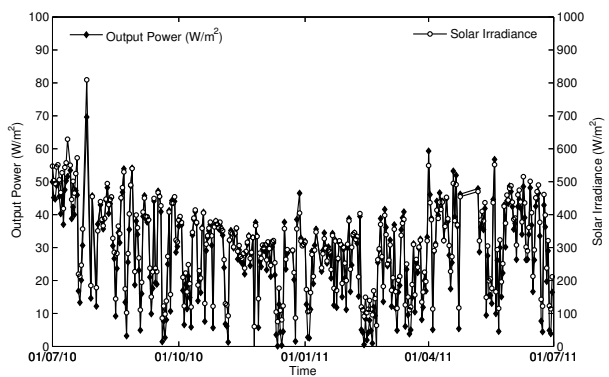


Fig. 2 Daily Averaged Solar Irradiance and Output Power from 01/07/2010 to 1/07/2011

(mm). The PV plates are fixed, inclined at an angle  $10^\circ$ , facing south-east. Under test conditions of cell temperature  $2.5^\circ\text{C}$  and Irradiance  $\text{AM1.5 } 1\text{ kW/m}^2$ , the max output power of each module is  $175\text{ W} \pm 5\%$ .

One Xantrex<sup>TM</sup> grid tie solar inverter (GT series) was used to convert DC to AC and connect the PV system to the grid. The system is connected to the grid from 5:00 to 20:00 every day. Start from 5:00, the solar energy is transformed into electrical energy and is provided to the grid. During the night time, the system is disconnected automatically at 20:00.

The data acquisition system was designed to operate automatically, and four physical parameters (radiation irradiance, PV cell temperature, output power, and wind speed) are monitored and recorded at one minute sampling intervals from July 1st 2010 to June 30th 2011.

### III. STATISTIC RESULTS BY CONVENTIONAL NEARBY POINT AVERAGING METHOD

A great deal of studies on daily or monthly averaged solar irradiance, output power and system energy efficiency for various solar PV systems have been done such as [4], [11]–[13]. It is obviously all these kind of statistical method is based on the time averaging on continuous nearby points.

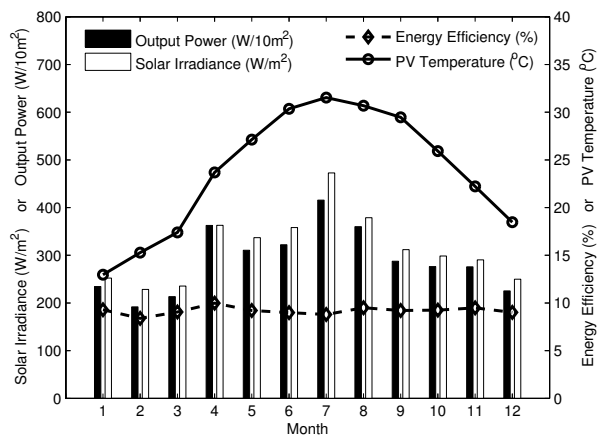


Fig. 3 Every Month Averaged Data from 01/07/2010 to 30/06/2011

Here, we would like to use this conventional method to analyze the present PV system to show the inherent limitation of this nearby point averaging method and the necessariness of introducing a new statistical method. Fig. 1 shows the results for solar irradiance and output power of the present PV system based on averaging nearby points in every hour from 01/03/2011 to 31/03/2011. By this hourly averaged statistical method, the minute to minute strong fluctuation is smoothed a little bit, but we can still see the tendency of increase from early morning to noon and decrease from noon to evening. Also we can not see the global level tendency, i.e. the month to month effect because the weak changing of month to month are covered by the strong changing of day to day due to weather changing. Fig. 2 shows the daily mean results for solar irradiance and output power for the present PV system from 01/07/2011 to 30/06/2011. There is a slightly change of daily mean results for both solar irradiance and output power for different months in a year, however, the day to day difference is still too strong to make the monthly difference tendency unclear to be seen. Also the distributions within a day are lost by daily average, we can not see the change due to time difference in a day any more. The monthly averaged results such as Fig.3 gives out the averaged changing for each month during one year. However, we can not see any changing due to time difference in a day, because this method covered the time effect by averaging the daily data before averaging the monthly data.

From the above discussion we can see that it is almost impossible for the conventional nearby point average statistical method to obtain a prediction model which can show both the changes due to time difference in a day and the changes of month to month over a year including the weather effects for solar irradiance, output power and the corresponding system energy efficiency of a solar PV system. Hence, in the next section we will introduce our novel typical day statistical method which will not average data of nearby points in the same day, hence the universal distribution rules in a day will be shown clearly.

## IV. TYPICAL DAY PREDICTION MODEL

## A. Typical Day Statistic Method

As discussed in last section, the conventional statistical results by nearby point averaging are effected dramatically by the weather conditions, which are very unpredictable. So we would like to build a novel typical day statistical model to obtain the statistical values for every minute in a typical day. Noting that, the typical day in the present study is not a real calendar day, and it is different from a typical clear day used by previous studies on solar PV systems by [9], [10]. The typical day in this paper is a statistical reference day, which represents the statistical characteristics including weather conditions for a period of time. The typical day is generally described by symbol  $D_p$ , where  $p$  represents the period of time it represents. Hence, a yearly typical day  $D_y$  is a statistical reference day for a period of one year and a monthly typical day  $D_m$  represents statistical characteristics of a period of one month.

In this model, the values for any variables at every minute in a typical day are obtained by averaging the variables for a period of days as:

$$Y(D_p, t) = \frac{1}{N_D} \sum_{d=1}^{N_D} Y(d, t) \quad (1)$$

where  $N_D = D_{end} - D_{start} + 1$  represents the number of total days in the time period presented by the typical day  $D_p$ . As shown in Eq. (1), we never average data from the same day, so the transient characteristics for minute to minute are kept. While the strong minute to minute fluctuations are smoothed in a typical day. Thus, by this method we can reveal the underline rules, whose phenomena are usually covered by the dramatically changes of minute to minute and day by day weather conditions. Unlike the conventional method which only provide the accumulated energy output in a typical clear day, this method can provide distribution of output power in a typical day.

The Gaussian curve have been applied to accurately predict peak oil production in the US by M. K. Hubbert [17], and it is still a popular method of estimate output of oil production today [18]. In the present study, we would like to apply similar method to analyze the data in a typical day, which have been obtained through Eq. (1). The Gaussian shape distribution of solar irradiance or output power in a typical day can be estimated by:

$$\hat{Y}(D_p, t) = \frac{\hat{Q}_{D_p}}{\sigma\sqrt{2\pi}} \exp\left[-\frac{(t - t_\mu)^2}{2\sigma^2}\right] \quad (2)$$

where,  $\hat{Y}$  is the estimated Gaussian function,  $t_\mu$  is the time at which the peak of the correlated Gaussian function occurs, and  $\sigma$  is a width parameter for the Gaussian curve. In the present study  $\sigma$  is in units of time (min).  $\hat{Q}$  is the estimated total integration value of  $\hat{Y}$  as:

$$\hat{Q}_{D_p} = \int_{t=-\infty}^{t=\infty} \hat{Y}(D_p, t) dt \quad (3)$$

The values of  $t_\mu$ ,  $\sigma$  and  $\hat{Q}_{D_p}$  can be adjusted iteratively by computer in order to minimize the Root Mean Squared Deviation (RMSD) between observed values and predicted by the Gaussian curve.

$$\text{RMSD} = \sqrt{\frac{1}{N} \sum_{i=1}^N (\hat{Y}(D_p, i) - Y(D_p, i))^2} \quad (4)$$

where  $N = (t_{end} - t_{start})/\Delta t$  represents the number of total point number integrated. In order to save computational time, the initial value of  $\hat{Q}_{inf}$  can be start from the real integrate value of  $Y(D_p, t)$ , i.e.

$$Q(D_p) = \int_{t=t_{start}}^{t=t_{end}} Y(D_p, t) dt. \quad (5)$$

where,  $t_{start}$  and  $t = t_{end}$  represent the start and stop time of the grid connected solar PV system in a typical day. The coefficient of determination  $R^2$  is defined as Eq. (6) to be a measure of how well the regression curve represents the data.

$$R^2 = 1 - \frac{\sum_{i=1}^N [Y(D_p, i) - \hat{Y}(D_p, i)]^2}{\sum_{i=1}^N [Y(D_p, i) - \bar{Y}(D_p, i)]^2} \quad (6)$$

From the statistical analysis method discussed above, we can get the optimal estimated Gaussian shape distribution of solar irradiance and output power for the PV system for the yearly and the 12 monthly typical day respectively.

## B. Prediction Model with Month to Month Effects for Solar Irradiance and Output Power

Duffie and Beckman [7] used the cosine function to express extraterrestrial solar radiation. It imply that the solar radiation is in a cosine shape periodic function of days in a year. Similar periodic ideas is used in the present prediction model to add the month to month effects on the Gaussian shape yearly typical day distribution. Thus, the prediction model is built in form of periodic Gaussian shape function derived from Eq. (2):

$$\hat{Y}(D_m, t) = \left\{ \frac{\hat{Q}_{D_y}}{\sigma\sqrt{2\pi}} \exp\left[-\frac{(t - t_\mu)^2}{2\sigma^2}\right] \right\} \times \left\{ 1.0 + \left[ \frac{\hat{Q}_{D(M_{max})} - \hat{Q}_{D(M_{min})}}{2\hat{Q}_{D_y}} \right] \cos\left[\frac{\pi(m - M_{max})}{6}\right] \right\} \quad (7)$$

where,  $\hat{Q}_{D_y}$ ,  $t_\mu$  and  $\sigma$  are obtained based on yearly typical day as described in section ???.  $\hat{Q}_{D(M_{max})}$  and  $\hat{Q}_{D(M_{min})}$  represent the maximum and minimum estimated monthly value of  $\hat{Q}_{D_m}$  respectively. Thus the amplitude of the monthly changing factor is:

$$\hat{A} = \frac{\hat{Q}_{D(M_{max})} - \hat{Q}_{D(M_{min})}}{2\hat{Q}_{D_y}} \quad (8)$$

## C. The Prediction Model for Energy Efficiency

The transient system energy efficiency at any date and time is defined as solar irradiance over the output power per unit area of the PV plates:

$$\eta(d, t) = \frac{P(d, t)}{R(d, t)} \quad (9)$$

Thus, we just use the simple estimated relation for the system energy efficiency as:

$$\hat{\eta}(D_m, t) = \frac{\hat{P}(D_m, t)}{\hat{R}(D_m, t)} \quad (10)$$

When Eq. (2) for solar irradiance and output power have been put into Eq. (10), the expression function of system energy efficiency is obtained as:

$$\begin{aligned} \hat{\eta}(D_m, t) &= \left[ \frac{(\hat{Q}_{D_y}/\sigma)_P}{(\hat{Q}_{D_y}/\sigma)_R} \right] \\ &\times \exp \left\{ -\frac{1}{2} \left[ \frac{(t - t_{\mu P})^2}{(\sigma_P)^2} - \frac{(t - t_{\mu R})^2}{(\sigma_R)^2} \right] \right\} \\ &\times \left\{ \frac{\hat{A}_P}{\hat{A}_R} + \frac{1 - \hat{A}_P/\hat{A}_R}{1 + \hat{A}_R \cos \left[ \frac{\pi(m - M_{max})}{6} \right]} \right\} \quad (11) \end{aligned}$$

where  $\hat{A}_P$  and  $\hat{A}_R$  are estimated amplitudes of output power and solar radiance respectively, and they can be obtained from Eq. (8).

## V. TYPICAL DAY STATISTIC ANALYSIS RESULTS

### A. Yearly Typical Day Results for Solar Irradiance and Output Power

Firstly, we would like to take the time period equal to one year to see the distributions for solar irradiance and output power of the present solar PV system in a yearly typical day. The mean values for output power in every minute of the yearly typical day is shown in Fig. 4 (b). In order to maximum the total energy output, we would like to find the optimal running time for the solar PV system in a year typical day, i.e. the optimal  $t_{start}$  and  $t_{end}$  in Eq. (5). The mean output power in a typical day is also plotted in Fig. 4(b) and zoom in near  $y = 0$  in Fig. 4(c). From Fig. 4(c), we can clearly see that the output power distribution curve meet the  $y = 0$  line on the optimal running time at  $t_{start}=06:30$  and  $t_{end}=18:33$  for the yearly typical day of the solar PV system in Macau. Also shown in 4(c), outside this range, the mean energy output is less than zero, which indicates the electrical flow direction is in the opposite direction. This also indicates that outside the optimal running range, the electrical energy will be transferred from the electrical grid to the grid-connected solar PV system, which should be avoided. Fig. 4(a) shows the accumulated output energy between the  $t_{start}=06:30$  and  $t_{end}=18:33$  in a yearly typical day. Thus the maximum possible accumulated output energy in a yearly typical day  $E(D_y)$  can be obtained

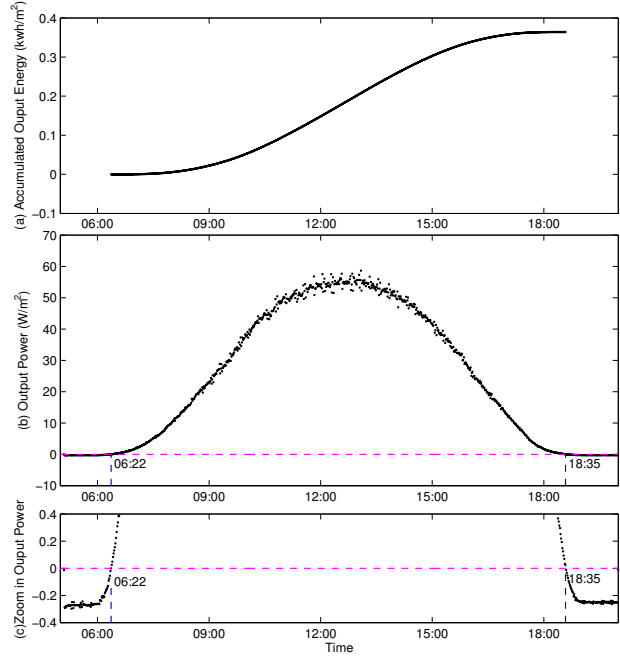


Fig. 4 Minute Distribution in a Yearly Typical Day for Radiation, Energy, Efficiency and PV Temperature

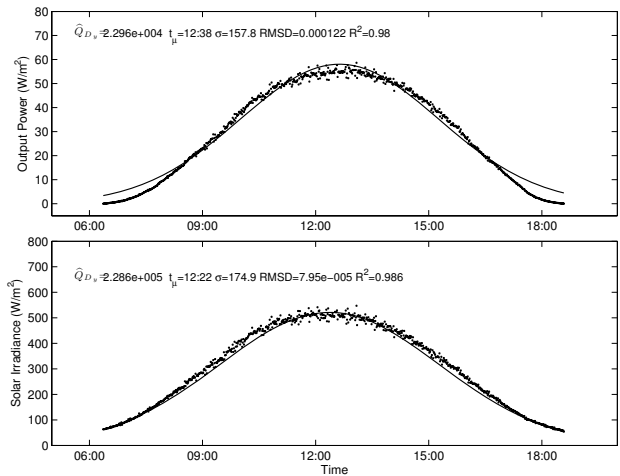


Fig. 5 Curve Fitting of Yearly Typical Day Data for Solar Radiation and Output Power by Gaussian Distribution

by integrating the output power  $P(D_y, t)$  from Eq. (5) as:

$$\begin{aligned} \max E(D_y) &= \int_{t=06:30}^{t=18:33} P(D_y, t) dt \\ &= 0.3465 \text{ (kWh/m}^2\text{)}. \quad (12) \end{aligned}$$

So the maximum possible accumulated output energy per unit PV area for a whole year (365 days) is  $126.48 \text{ kWh/m}^2$ .

The method discussed in section ?? is applied to obtain the three governing parameters in the Gaussian distribution of Eq. (2), i.e.  $\hat{Q}_{D_y}$ ,  $t_{\mu}$  and  $\sigma$ . The comparison of the Gaussian shape distribution of solar irradiance and output power are shown

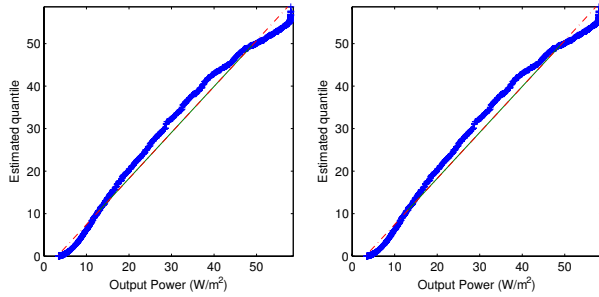


Fig. 6 Quantile-quantile Plot for Solar Irradiance and Output power

in bottom and top of Fig. 5 respectively. From Fig. 5, we can see that both have a nice Gaussian form distribution with  $R^2$  equals to 0.985 and 0.978 for solar irradiance and output power respectively, which shows they are both acceptable for Gaussian fit. For the output power the lower values which are nearly zero output are a bit higher than the Gaussian estimated values. The peak time of the solar irradiance is  $t_\mu=12:23$ , while the peak time of the output power is 17 minutes later than that of the solar irradiance. Also the yearly typical day value of  $\sigma$  of solar radiation is about 174 mins which is about 20 mins wider than the  $\sigma$  of the output power. The estimated  $\hat{Q}_{D_y}$  for solar irradiance is about 10 times of  $\hat{Q}_{D_y}$  for output power, which also show that for a typical day, the averaged system energy efficiency is about 10%. Quantile-quantile Plot for Solar Irradiance and Output power have been plotted in Fig. 6, which also show that most of the estimated value from Gaussian shape distribution match the data of the typical day very well, except those few at ending where values are near to zero. Also it show that for the output power near zero the estimated values are slightly higher than the real ones.

### B. Monthly Typical Day Results for Solar Irradiance and Output Power

Simpler as the yearly typical day analysis method, if we pick the time period as long as one month, we can obtain monthly typical day static analysis results for each month respectively. Table I and Table II give out the iteration results for output power and solar irradiance on the site of Macau and the output power of the present grid connected PV system. From Table I, we can see that the radiation and output power have maximum  $\hat{Q}_{D_m}$  values in July, which agrees with the monthly averaged solar irradiance in Macau calculated by [12], [14]. In Fig. 7, the monthly typical day results for month 2,5,7 and 12 are compared together, which give a clear picture of how the solar irradiance, output power and accumulated output energy distribution various with seasons.

### C. Monthly Typical Day Correlation for Solar Irradiance and Output Power

For the year from July 2010 to June 2011 referring to Fig. 5, Table I and Table II we can get the simplified periodic form of solar irradiance and output power in a typical day of any

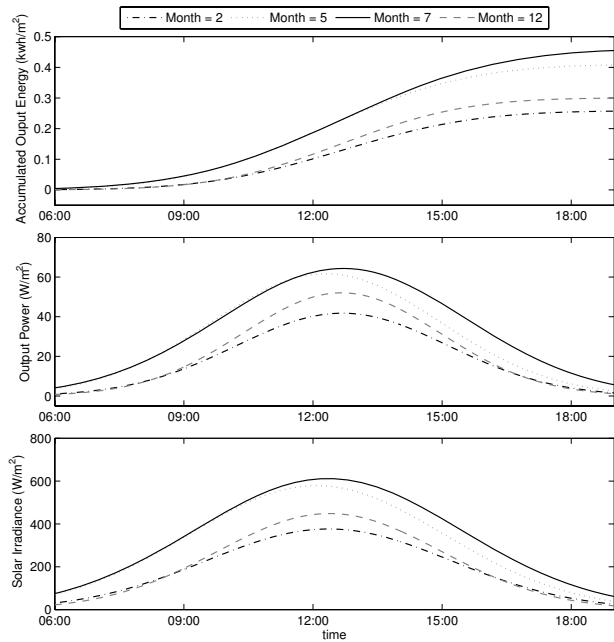


Fig. 7 Monthly Typical Day Distribution Correlated by Gaussian Curves with Minimum RMSD

TABLE I  
TYPICAL DAY GAUSSIAN PARAMETERS FOR OUTPUT POWER

Month	Output Power			
	$\hat{Q}_{D_m} (\times 10^4)$	$t_\mu$	$\sigma(\text{min})$	$R^2$
1	1.9068	13:03	137.9	0.9714
2	1.5497	12:41	148.0	0.9492
3	1.9442	12:44	147.6	0.9722
4	2.7160	12:50	141.5	0.9133
5	2.5122	12:19	162.4	0.9424
6	2.6939	12:32	164.5	0.9519
7	2.7670	12:43	171.4	0.9474
8	2.7285	12:50	171.1	0.9426
9	2.5318	12:36	165.7	0.9639
10	2.5062	12:21	146.7	0.9708
11	2.2960	12:28	142.9	0.9644
12	1.8026	12:40	138.1	0.9701
Yearly	2.2960	12:38	157.8	0.9796

TABLE II  
TYPICAL DAY GAUSSIAN PARAMETERS FOR SOLAR IRRADIANCE

Month	Solar Irradiance			
	$\hat{Q}_{D_m} (\times 10^5)$	$t_\mu$	$\sigma(\text{min})$	$R^2$
1	1.7884	12:45	159.3	0.9542
2	1.6111	12:22	170.8	0.9285
3	1.9081	12:36	169.1	0.9657
4	2.7473	12:35	159.8	0.9137
5	2.6334	12:05	178.0	0.9406
6	2.8495	12:15	182.2	0.9358
7	2.8496	12:21	185.9	0.9560
8	2.6515	12:33	182.2	0.9487
9	2.4959	12:18	177.9	0.9605
10	2.4241	12:08	162.6	0.9693
11	2.1465	12:10	159.2	0.9591
12	1.7533	12:23	156.0	0.9614
Yearly	2.2864	12:22	174.9	0.9865

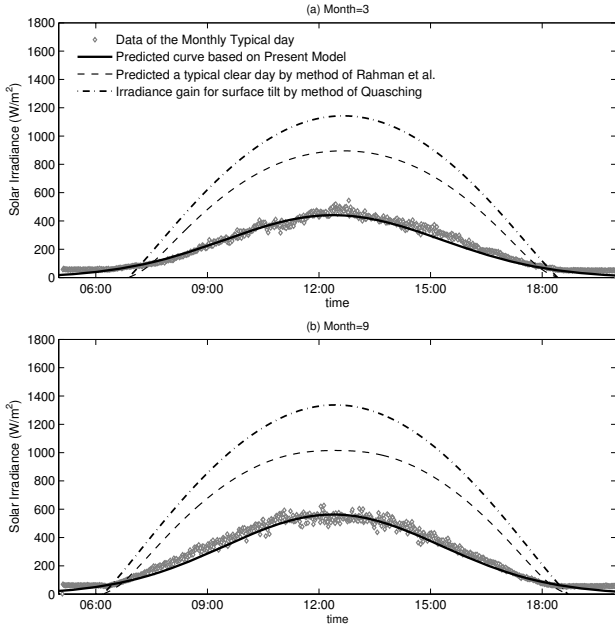


Fig. 8 Comparison of Predicted Solar Irradiance in March and September by the Present Model with Measured Data, Model of Rahman et al. [10] and model of Quasching [6] respectively

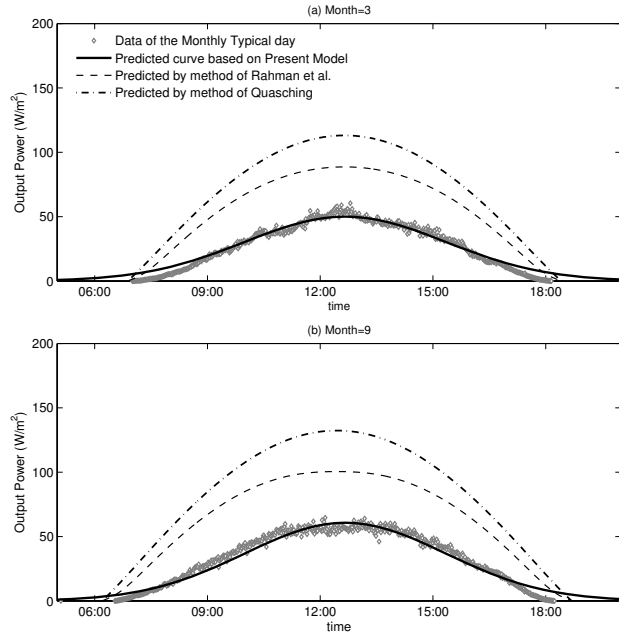


Fig. 9 Comparison of Predicted Energy Efficiency in a Typical Day to Data, Mean Real Values and Fixed Value Used by Rahman et al. [10]

month of a year in form of Eq. (7):

$$\hat{R}(D_m, t) = \left\{ \frac{2.193 \times 10^5}{174.3\sqrt{2\pi}} \exp \left[ -\frac{(t-12:23)^2}{2(174.3)^2} \right] \right\} \times \left\{ 1.0 + 0.2824 \cos \left[ \frac{\pi(m-7)}{6} \right] \right\} \quad (W/m^2) \quad (13)$$

$$\hat{P}(D_m, t) = \left\{ \frac{2.227 \times 10^4}{160.5\sqrt{2\pi}} \exp \left[ -\frac{(t-12:40)^2}{2(160.5)^2} \right] \right\} \times \left\{ 1.0 + 0.2609 \cos \left[ \frac{\pi(m-7)}{6} \right] \right\} \quad (W/m^2) \quad (14)$$

To validate the effectiveness of the the present correlations for solar irradiance Eq. (13) and output power Eq. (14) in a typical day for any months, March and September are selected and compared to previous studies. Fig. 8 and Fig. 9 shows the comparison of solar irradiance and the output power to data of typical day and models of [6] and [10] respectively. The models of [6] and [10] are all based on a clear day, so their prediction results for both solar radiance and the output power are larger than the real value for a typical day which include the weather conditions. The present model is obviously better for the prediction of both solar radiance and the output power for a real system including site weather conditions.

#### D. Monthly Typical Day Correlation for Energy Efficiency

Also based on Fig. 5, Table I and Table II, or Eq. (13) and (14) we can get the coefficients for Eq. (11). The correlation for the energy efficiency of the present system is given as:

$$\hat{\eta}(D_m, t) = 0.1103 \exp \left\{ -\frac{1}{2} \left[ \frac{(t-12:40)^2}{(160.5)^2} - \frac{(t-12:23)^2}{(174.3)^2} \right] \right\} \times \left\{ 0.9239 + \frac{0.0761}{1+0.2824 \cos \left[ \frac{\pi(m-7)}{6} \right]} \right\} \quad (15)$$

Fig. 10 shows the present prediction results based on correlations Eq. (15) compared to Typical Day transient values of the system energy efficiency of the real system. Also the mean value of the system efficiency and the fixed value used by [10] are plotted in dash and dash dot lines respectively. The picture show that during most of the day time, from 8:30 to 17:00, the correlation of Eq. (15) gives out a pretty good transient efficiency. The discrepancy of start and ending time are due to errors introduced by the Gaussian distribution of the output power for those near zero values. Also it is the first transient prediction model for energy efficiency in a monthly Typical Day, which does not depend on other measurement data exception solar irradiance and output power. Because most of the solar energy are concentrated in time period from 8:30 to 17:00, the present correlation provide a practical way to prediction the system efficiency for the real on site solar PV system.

## VI. CONCLUSIONS

A novel periodic Gaussian shape typical day prediction model obtained by averaging discontinuous data has been built and validated by the measured data of a grid-connected PV system in Macau. The advantage of the present model is that the dynamical effects due to time difference in a day are kept and the day to day uncertainty due to weather

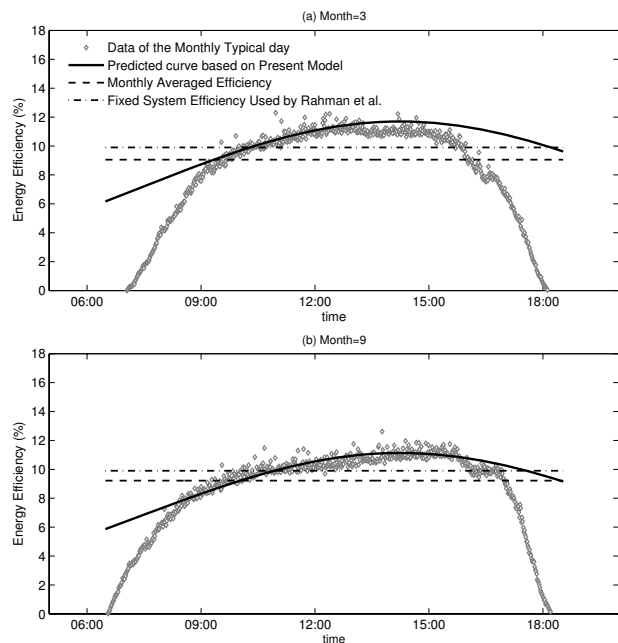


Fig. 10 Comparison of Predicted Energy Efficiency in a Typical Day to Data, Mean Real Values and Fixed value used by Rahman et al. [10]

changing are smoothed but still included. Gaussian shape dynamical distributions for solar irradiance and output power in a yearly or monthly typical day have been obtained by this Typical Day statistical method. Based on the yearly typical Day statistical analysis results, we obtained the maximum possible accumulated output energy in a year with on site climate conditions and the corresponding optimal running time. Periodic Gaussian shape prediction models for solar irradiance, output energy and system energy efficiency have been built and their coefficients have been determined based on the yearly, maximum monthly and minimum monthly typical day Gaussian distribution parameters. Practical monthly based periodic Gaussian form of correlations for solar irradiance, output power and the system energy efficiency for every minute of a monthly typical day have been compared favorably with monthly typical day data of the PV system in Macau and proved to be an improvement than previous models. The present periodic Gaussian form prediction correlations are also expected to more practical for design and evaluation of solar PV systems.

#### ACKNOWLEDGMENTS

This study was supported by the Multi-Year Research Grant (MYRG) MYRG151(Y1-L2)-FST11-SY and the Start-Up Research Grant (SRG) SRG009-FST11-YS of the Macau University. Also thanks the Information and Communication Technology Office (ICTO) of University of Macau.

#### REFERENCES

- [1] Mondal, M.A.H. and Islam, A.K.M.S., (2011), "Potential and viability of grid-connected solar PV system in Bangladesh," *Renewable Energy*, 36, pp. 1869-1874.
- [2] Green, M. A. (2004), "Recent developments in photovoltaics," *Solar Energy*, 76, pp. 3-8.
- [3] Li, Y.Z., He, Lin, and Nie, R.Q., (2009), "Short-term forecast of power generation for grid-connected photovoltaics system based on advanced Grey-Markov Chain," *International Conference on Energy and Environment Technology*, Taj Chandigarh, India, pp. 275-278.
- [4] Mellit, A., Kalogiou, S.A., Shaari, S. and Arab A.H., (2008), "Methodology for prediction sequences of mean monthly clearness index and daily solar radiation data in remote areas: Application for sizing a stand-alone PV system," *Journal of Solar Energy Engineering*, 127, 4, pp. 324-332.
- [5] Al-Karaghoul, A. and Kazmerski, L.L., (2010), "Optimization and life-cycle cost of health clinic PV system for a rural area in southern Iraq using HOMER software," *Solar Energy*, 84, pp. 710-714.
- [6] Quasching, V. (2005), "Understanding renewable energy systems," *Carl Hanser Verlag GmbH and Co KG*, pp. 44-66.
- [7] Duffie, J.A. and Beckman, W.A. (1980), "Solar Engineering of Thermal Processes," *New York: John Wiley and Sons*, pp. 1-27.
- [8] Nott, G., Lazarov, V. and Stoyanov, L., (2010), "Optimal sizing of a grid-connected PV system for various PV module technologies and inclinations, inverter efficiency characteristics and locations," *Renewable Energy*, 35, pp. 541-554.
- [9] Merino G.G., Jones, D., and Stetson, L.E. (2000), "Performance of A Grid-Connected Photovoltaic System Using Actual and Kriged Hourly Solar Radiation," *American Society of Agricultural Engineers-Transactions of ASAE*, 43, 4, pp. 1011-1018.
- [10] Rahman, M. H., Nakayama, J., Nakamura, Y. and Yamashiro, S., (2004), "A viable grid-connected PV-ECS system with load leveling function using a day-ahead weather forecast," *International Conference on Power System Technology-POWERCON*, Singapore, pp.21-24 November, 2004.
- [11] Perpinan, O. (2009), "Statistical analysis of the performance and simulation of a two-axis tracking PV system," *Solar Energy*, 83, pp. 2074-2085.
- [12] Chow, T.T., Chan, A.L.S., Fong, K.F. and Lin Z., (2006), "Some perceptions on typical weather year-from the observations of Hong Kong and Macau," *Solar Energy*, 80, 4, pp. 459-467.
- [13] Li, D.H.W., Cheung, K.L., Lam, K.L., and Chan W.W.H., (2011), "A study of grid-connected photovoltaic (PV) system in Hong Kong," *Applied Energy*, doi:10.1016/j.apenergy.2011.01.054.
- [14] Chow, T.T. and Chan, A.L.S., (2004), "Numerical study of desirable solar-collector orientations for the coastal region of South China," *Applied Energy*, 79, pp. 249-260.
- [15] Newland, F. J., (1989), "Study of solar radiation models for the coastal region of South China," *Solar Energy*, 43, 4, pp. 227-235.
- [16] Aynonpe, L.M., Duffy, A., McCormack, S.J., and Conlon, M. (2011), "Measured performance of a 1.72 kW rooftop grid connected photovoltaic system," *Energy Conversion and Management*, 52, 4, pp. 816-825.
- [17] Hubbert, M.K., (1956), "Nuclear energy and fossil fuels," *Am. Petrol. Inst. Drilling and Production Practice*, pp. 7-25.
- [18] Abrams, D. M. and Wiener, R. J. (2010), "A model of peak production in oil fields," *American Journal of Physics*, 78, 1, pp. 24-27.